Catalysis Letters Vol. 102, Nos. 3–4, August 2005 (© 2005)
DOI: 10.1007/s10562-005-5861-7

Reaction performance and characterization of Co/Al_2O_3 Fischer–Tropsch catalysts promoted with Pt, Pd and Ru

Dongyan Xu, Wenzhao Li*, Hongmin Duan, Qingjie Ge, and Hengyong Xu

Natural Gas Utilization and Applied Catalysis Laboratory, Dalian Institute of Chemical Physics, Chinese Academy of Sciences, Dalian 116023, P. R. China

Received 11 January 2005; accepted 13 March 2005

A series of noble metal (Pt, Ru or Pd) promoted Co/Al_2O_3 catalysts were prepared by sequential impregnation method. The catalysts were characterized by XRD, TPR, H_2-TPD and TPSR techniques, and their catalytic performance in Fischer–Tropsch synthesis was investigated in a fixed-bed reactor. The results of activity measurements show that the addition of small amounts of noble metal greatly improved the activity of the Co/Al_2O_3 catalyst. TPR experimental results demonstrate that hydrogen spillover from the noble metal to cobalt oxide clusters facilitated the reduction of cobalt oxide and, thus significantly increased the reducibility of Co/Al_2O_3 catalyst. The presence of noble metal increased the amount of chemisorbed hydrogen and weakened the bond strength of Co–H. TPSR results indicate that CO was adsorbed in a more reactive state on the promoted catalysts.

KEY WORDS: Fischer–Tropsch synthesis; cobalt; alumina; noble metal; hydrogen spillover.

1. Introduction

Fischer–Tropsch synthesis (FTS) has regained interest for the conversion of natural gas or coal-bed methane to high-boiling waxy hydrocarbons that may be converted to fuels by hydrocracking or to lubricating base oil by hydroisomerization. For gas-to-liquid (GTL) technology, supported cobalt catalysts are the preferred catalysts due to their high activity, selectivity for linear hydrocarbons, low activity for the water gas shift (WGS) reaction, and lower price compared to noble metals [1].

Although alumina is often used as support for cobalt catalysts due to its high resistance to attrition in the continuously stirred tank reactor or slurry bubble column reactor and its favorable ability to stabilize a small cluster size [2,3], the cobalt alumina catalysts have a limited reducibility due to strong interaction between the support and the cobalt oxides [3,4]. Previous studies have shown that a small amount of noble metals, such as Ru, Pt or Re, can promote the reduction of cobalt alumina catalysts [2,4–10]. However, it is not clear how noble metal promotes the FTS reaction in addition to promote the reduction of cobalt oxides. It could, therefore, facilitate the design of active cobalt alumina catalyst to understand how noble metal modifies catalyst properties.

The purpose of this study is to investigate the effect of noble metal (Pt, Pd, or Ru) upon $Co/\gamma\text{-}Al_2O_3$ catalyst characteristics and performance. X-ray diffraction (XRD), temperature programmed reduction (TPR), temperature programmed desorption (TPD), temperature programmed surface reaction (TPSR) and BET surface area measurement were used to characterize the catalysts. The catalytic performances of these catalysts were investigated for FTS with syngas containing CO_2 and N_2, which is produced by the integrated air partial oxidation with H_2O–CO_2 reforming of natural gas [11].

* To whom correspondence should be addressed.
E-mail: wzli@dicp.ac.cn

2. Experimental

2.1. Catalyst preparation

The cobalt catalyst was prepared by incipient wetness impregnation of $\gamma\text{-}Al_2O_3$ (Shandong Alumina Plant, China, BET surface area 248 m^2/g, average pore volume 0.45 ml/g) support with aqueous solution of cobalt nitrate ($Co(NO_3)_2 \cdot 6H_2O$), followed by drying at 393 K for 12 h and calcination in air at 673 K for 8 h. The noble metal (Pt, Pd or Ru) promoted catalysts were prepared by subsequently impregnating the $Co/\gamma\text{-}Al_2O_3$ catalyst with the aqueous solution of hydrogen hexachloroplatinate hexahydrate ($H_2PtCl_6 \cdot 6H_2O$), palladium chloride ($PdCl_2$) and ruthenium chloride trihydrate ($RuCl_3 \cdot 3H_2O$), respectively. After promoter addition, the catalysts were then dried overnight and calcined at 673 K for 4 h. All the promoted catalysts contain 12 wt% Co and 0.5 wt% noble metal. For clarification purposes on how noble metal addition affects catalyst performance, supported noble metal catalysts were also prepared by the same impregnation method.

2.2. Catalyst characterization

2.2.1. BET surface area and porosity measurements

The BET surface area, pore volume and average pore diameter were determined by N_2 physisorption at 77 K

using a Micromeritics ASAP-2010 automated system. Prior to the measurements, all the catalyst samples were outgassed at 623 K for 2 h.

2.2.2. X-ray diffraction (XRD)

XRD measurements were performed with a Rigaku D/max-rB X-ray diffractometer using Cu K_α radiation. Calcined catalyst samples were used for the XRD measurements. The average particle size of Co_3O_4 was calculated from line broadening analysis of the most intense Co_3O_4 line ($2\theta = 36.9°$) using the Scherrer formula. The Co_3O_4 particle sizes of the calcined catalysts were then converted to the corresponding cobalt particle diameters of the reduced catalysts according to the relative molar volumes of metallic cobalt and Co_3O_4 using the following equation [12]:

$$d(\mathrm{Co}^0) = 0.75 \cdot d(\mathrm{Co_3O_4}).$$

Then, the cobalt metal dispersion (D) can be calculated from the average cobalt metal particle size, assuming spherical uniform metal particles with site density of 14.6 atoms/nm^2, by using the following formula [13]:

$$D = 96/d(D = \%, d = \mathrm{nm}).$$

2.2.3. Temperature programmed reduction (TPR)

TPR experiments were carried out in a quartz microreactor. The calcined catalyst sample (40 mg) was first purged with high purity Ar flow at 623 K for 0.5 h to remove traces of water, followed by cooling to room temperature. TPR was performed by heating the samples from room temperature to 1173 K at a rate of 10 K/min, in a 5% H_2/Ar mixture (30 ml/min). The water produced during the reduction was removed by passing the outlet gas through a trap cooled by dry ice in ethanol. A thermal conductivity detector (TCD) was used to measure H_2 consumption quantitatively. In order to evaluate the fraction of reduced cobalt during catalyst activation, TPR was also performed for the catalyst after an *in situ* reduction at 673 K for 8 h in pure H_2 flow. Then, the TPR spectrum was integrated and the amount of consumed hydrogen determined by comparing its area to the area of the standard sample of Ag_2O.

2.2.4. H_2 Temperature-programmed desorption (H_2-TPD)

H_2-TPD experiments were performed in the same apparatus as the TPR experiments. The catalyst sample (0.1 g) was reduced using pure hydrogen at 673 K for 8 h and then cooled to room temperature under flowing hydrogen. This reduction condition is same as that utilized for activation in reaction tests. The sample was held at 298 K for 1 h under flowing argon to remove physisorbed and/or weakly bound species. TPD was performed by heating the sample from room temperature to 973 K using a ramp rate of 10 K/min under a flow of argon. Desorbed gases were monitored by a thermal conductivity detector.

2.2.5. Temperature programmed surface reaction (TPSR) of adsorbed CO

TPSR experiments of adsorbed CO were performed using Micromeritics Autochem 2910 instrument at atmospheric pressure. Prior to the measurement, the catalyst sample (0.2 g) was reduced by flowing hydrogen at 673 K for 2 h. Following the reduction, the sample was purged with flowing He at 673 K for 0.5 h and then cooled under flowing He to 298 K. CO was adsorbed by flowing a CO/He (5% v/v) mixture at 298 K for 1 h. Then, the sample was purged with Ar flow for 30 min to remove physisorbed CO. Finally, the temperature was linearly increased from 298 to 773 K at a heating rate of 10 K/min under a H_2/Ar (10% v/v) flow. The fragments $m/e = 2$, 16, 18, 28 and 44 were recorded by a quadrupole mass spectrometer (Ominister 300).

2.3. Catalyst testing

The FTS reaction was performed in a fixed-bed stainless steel reactor using a nitrogen-diluted syngas mixture that was produced by an integrated air partial oxidation with CO_2–H_2O reforming of CH_4. The composition of the syngas mixture is $H_2/CO/N_2/CH_4/CO_2 = 2.08/1.00/2.06/0.03/0.47$ (molar ratio). The nitrogen contained in the syngas mixture was used as an internal standard to determine the CO conversion. The calcined catalyst (1 g) was loaded into the isothermal zone of the reactor. The reaction temperature was measured by a thermocouple inserted into the catalyst bed. Prior to reaction, the catalyst was reduced *in situ* in a flow of pure hydrogen at 673 K for 8 h under atmospheric pressure. After catalyst activation, the reactor temperature was decreased to 433 K in flowing H_2 and the syngas mixture was introduced. Then, the reactor pressure was increased to 2.0 MPa and the temperature slowly increased to 503 K. Gaseous products were analyzed with on-line chromatographs (Shimadzu GC-8A) equipped with thermal conductivity detector (TCD) and flame ionization detector (FID). N_2, CO, CO_2 and CH_4 were analyzed on the TCD after separation by a Carbosieve column. Light hydrocarbons (C_1–C_4) were separated by a Porapack-Q column and detected on the FID.

3. Results and discussion

3.1. Catalytic activity and selectivity

The noble metal promoted Co/Al_2O_3 catalysts have been tested for FTS at 503 K and 2.0 MPa. The CO conversions and hydrocarbon selectivities (mole carbon base) of various catalysts are summarized in table 1. The

Table 1
Catalytic performances of unpromoted and promoted Co/Al_2O_3 catalysts for FTS[a]

Catalyst	CO conversion (%)	CO_2 selectivity (%)	Hydrocarbon selectivity (%)				
			C_1	C_2	C_3	C_4	C_5^+
Co/Al_2O_3[b]	6.4	~0	27.5	4.8	6.4	9.1	52.2
$Co–Pt/Al_2O_3$	61.3	9.1	15.6	1.4	2.9	3.6	67.4
$Co–Ru/Al_2O_3$	58.3	9.3	15.5	1.3	2.8	3.1	68.0
$Co–Pd/Al_2O_3$	33.1	7.9	24.2	2.4	4.3	3.7	57.5
Pt/Al_2O_3	1.6						
Ru/Al_2O_3	8.4	~0	5.2	0.3	0.9	0.8	92.8
Pd/Al_2O_3	1.0						

[a] Reaction conditions: 503 K, 2.0 MPa, 500 h^{-1}.
[b] Data obtained at the reaction temperature of 513 K.

unpromoted Co/Al_2O_3 catalyst was found to exhibit extremely low activity even at the reaction temperature of 513 K. However, the activity for FTS was greatly enhanced when a small amount of noble metal was added to Co/Al_2O_3. According to table 1, the catalytic activities of cobalt catalysts follow the order $Co–Pt/Al_2O_3$ > $Co–Ru/Al_2O_3$ > $Co–Pd/Al_2O_3$ > Co/Al_2O_3. Although Ru is thought to be the most active metal for FTS, the CO conversion of Ru/Al_2O_3 is only 8.4% because of the low loading. Compared with Ru/Al_2O_3, the Pt/Al_2O_3 and Pd/Al_2O_3 catalysts displayed much lower CO conversions. These results reveal that the high activities of the promoted Co/Al_2O_3 catalysts are ascribed to the pronounced catalytic synergistic effect between cobalt and noble metals. In addition, the addition of noble metal to Co/Al_2O_3 was found to decrease the methane selectivity and increase C_5^+ selectivity.

3.2. Catalyst characterization

3.2.1. BET surface area and porosity data

Table 2 shows the results of surface area measurements by nitrogen adsorption at 77 K. Because a loading of 12% Co metal is equivalent to about 15% Co_3O_4 by weight, the BET surface area of the Co/Al_2O_3 catalyst should be approximately $0.85\times 248 = 211$ m^2/g in theory. The measured value (170 m^2/g), however, is obviously lower than the theoretical value, indicating that some pore blockage by cobalt oxide clusters occurred. For the noble metal promoted catalysts, the measured values are much closer to the theoretical value than Co/Al_2O_3 catalyst, suggesting that a second calcination after noble metal addition caused further distribution of Co_3O_4 on the surface of Al_2O_3, and hence decreased the pore blockage.

Table 2
BET surface area and porosity data

Support/catalyst	Surface area (m^2/g)	Average pore diameter (nm)	Pore volume (cm^3/g)
γ-Al_2O_3	248	7.2	0.45
Co/Al_2O_3	170	6.8	0.30
$Co–Pt/Al_2O_3$	180	6.8	0.31
$Co–Ru/Al_2O_3$	205	6.8	0.34
$Co–Pd/Al_2O_3$	194	6.6	0.32

3.2.2. X-ray diffraction

XRD patterns for the calcined unpromoted and noble metal promoted Co/Al_2O_3 catalysts are shown in figure 1. For reference, the XRD pattern of Al_2O_3 support is also given. The unpromoted and promoted Co/Al_2O_3 catalysts exhibited almost identical XRD patterns. The diffraction peaks at 18.9°, 31.3°, 36.8°, 44.9°, 59.3°, and 65.3° correspond to different crystal planes of Co_3O_4. No peaks attributed to Pt, Pd, and Ru oxides were observed due to their low contents in the catalysts.

Table 3 shows the average Co_3O_4 crystallite sizes calculated using the Scherrer formula. The average

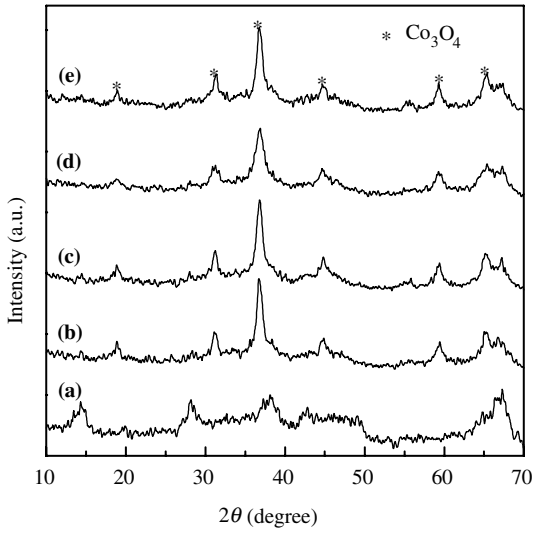

Figure 1. XRD patterns of Al_2O_3 and the calcined Co/Al_2O_3 catalysts promoted with different noble metals. (a) Al_2O_3; (b) Co/Al_2O_3; (c) $Co–Ru/Al_2O_3$; (d) $Co–Pt/Al_2O_3$; (e) $Co–Pd/Al_2O_3$.

Table 3
Particle diameters and dispersions of different catalysts.

Catalyst	Particle diameter (nm)		Dispersion (%)
	d (Co_3O_4)	d (Co)	
Co/Al_2O_3	10.1	7.6	12.6
$Co–Pt/Al_2O_3$	7.3	5.5	17.5
$Co–Ru/Al_2O_3$	8.0	6.0	16.0
$Co–Pd/Al_2O_3$	9.8	7.4	13.0

Co_3O_4 crystallite size of the unpromoted Co/Al_2O_3 catalyst is approximately 10.1 nm corresponding to 7.6 nm when reduced to the Co metal. After the addition of small amounts of noble metal, the average Co_3O_4 crystallite size decreased to some extent. These changes in average Co_3O_4 crystallite size after noble metal addition may be caused by the second calcination, which enhanced the interaction between Co_3O_4 and support and the contact between Co and noble metal. The cobalt dispersions estimated from XRD are presented in table 3.

3.2.3. Temperature-programmed reduction

The reduction profiles of various catalysts are shown in figure 2. For unpromoted Co/Al_2O_3 catalyst, two peaks are located at 652 K and between 723 and 1173 K (maximum at 932 K), respectively. Although extensive TPR studies on Co/Al_2O_3 have been made, there still exist different opinions about the attribution of the reduction peaks. Some researchers suggested that the low temperature peak is ascribed to the two-step reduction of relatively large crystalline Co_3O_4 particles to Co^0 via CoO [5,14,15]. Whereas others proposed that the low temperature peak is ascribed to the reduction of Co_3O_4 to CoO, though a fraction of the peak may likely correspond to the reduction of the large, bulk-like CoO species to Co^0 [7,16]. While the precise identity of the species is not clear, most researchers are in agreement that the broad high temperature peak is attributed to the reduction of highly dispersed cobalt surface species strongly interacting with Al_2O_3. It should be mentioned that the H_2 consumption is still continued at 1173 K in the TPR profile, implying that some cobalt aluminate ($CoAl_2O_4$) might be formed, the reduction of which occurs only above 1073 K [17]. This cobalt aluminate is possibly caused by the diffusion of Co^{2+} ions into the Al_2O_3 support where they may occupy tetrahedral or octahedral lattice sites [18]. Because both $CoAl_2O_4$ and Co_3O_4 have cubic spinel structure with almost same XRD patterns, it is difficult to effectively detect the phase of $CoAl_2O_4$ for the calcined catalysts.

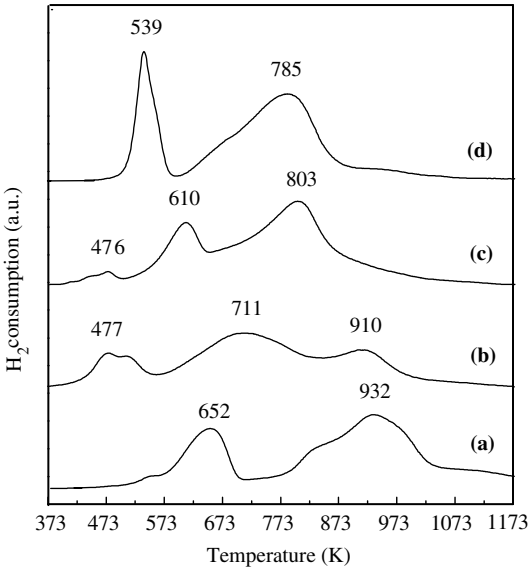

Figure 2. TPR profiles of the unpromoted and promoted Co/Al_2O_3 catalysts. (a) Co/Al_2O_3; (b) $Co–Pd/Al_2O_3$; (c)$Co–Ru/Al_2O_3$; (d) $Co–Pt/Al_2O_3$.

As shown in figure 2, both peaks have markedly shifted to lower temperatures after the addition of Pt to Co/Al_2O_3. This indicates that the presence of Pt can catalyze the reduction of both Co_3O_4 and cobalt oxide species interacting with the support. It was found that the first peak temperature of $Co–Pt/Al_2O_3$ is very close to that of Pt/Al_2O_3 catalyst (not shown). Therefore, the first peak of $Co–Pt/Al_2O_3$ is due to the reduction of Pt oxide and Co_3O_4. Similarly, samples promoted with Pd and Ru showed lower reduction temperatures in comparison with the unpromoted sample. However, some different characteristics on the TPR spectra were observed. For $Co–Ru/Al_2O_3$ catalyst, two resolved low temperature peaks are present at 476 and 610 K, respectively. It has been suggested that the high mobility of Ru can induce the interactions of cobalt and ruthenium and the formation of mixed Co–Ru oxides [19]. Thus, it can be deduced that the small reduction peak located at 476 K correspond to the reduction of RuO_2 and the Co_3O_4 particles that have intimate contact with RuO_2, while the peak located at 610 K is possibly due to the reduction of the Co_3O_4 particles that have no direct contact with RuO_2. Based on these results, it is speculated that the adsorbed hydrogen is first dissociated on the reduced noble metal clusters and converted to active hydrogen, which can migrate to the neighboring cobalt oxide clusters directly or to the remote cobalt oxide species via the surface of Al_2O_3. In brief, hydrogen spillover from the reduced Pt (Pd or Ru) metal not only facilitates the reduction of Co_3O_4 but also the reduction of cobalt surface species interacting with the support, and consequently increases the amount of available active cobalt metal sites for catalytic reaction.

To investigate the fraction of reduced cobalt during catalyst activation, a modified TPR method that consists of a standard reduction in pure H_2 at 673 K for 8 h as used in the catalyst testing and followed by a standard TPR (up to 1200 K) was used in this study.

The H_2 consumptions in the TPR are listed in table 4. It is expected that, after the standard reduction at 673 K for 8 h, Co_3O_4 has been completely reduced to CoO. Recent XANES study has shown that the broad high temperature peak of Co/Al_2O_3 catalyst is due to the reduction of small CoO clusters interacting with the support [16]. Therefore, the H_2 consumptions of the catalysts after standard reduction could be assumed to correspond to the reduction of remaining CoO in the catalysts. Based on this assumption, the rough reducibilities of various catalysts during activation were calculated. The results show that the addition of noble metals significantly increases the reducibility of Co/Al_2O_3 catalyst. Thus, it is reasonable to conclude that the improvements in catalytic performances of the promoted catalysts are closely related to the enhancements of reducibility.

3.2.4. Temperature-programmed desorption

All H_2-TPD spectra of the unpromoted and promoted Co/Al_2O_3 catalysts show two major peaks: a low temperature peak (<623 K) and a high temperature peak (>673 K) that could be attributed to different adsorbed states of hydrogen (see figure 3). According to the previous studies on Co/Al_2O_3 [20] and $CoRu/SiO_2$ [21] catalysts, the low temperature peak is ascribed to chemisorbed hydrogen on the metal surface. The high temperature desorption peaks were often observed on the H_2-TPD spectra of various catalysts, although the peak temperatures may be different. Hilmen *et al.* [20] suggested the high temperature peak located at about 800 K is more likely caused by desorption of spillover hydrogen from the support. Similarly, other authors also proposed that the high temperature desorption peaks of Pt/Al_2O_3 [22], Ru/Al_2O_3 [23] and Rh/SiO_2 [24] are assigned to spillover hydrogen from the metal particles to the support surface. Therefore, the low temperature peaks and high temperature peaks displayed in figure 3 are most likely ascribed to chemisorbed hydrogen on the metal surface and spillover hydrogen on the support, respectively.

Table 4
Hydrogen consumptions and reducibilities of different catalysts

Catalyst	H_2 consumption (mmol/g-cat)	Reducibility (%)
Co/Al_2O_3	0.74	63.7
$Co–Pt/Al_2O_3$	0.28	86.3
$Co–Ru/Al_2O_3$	0.43	78.9
$Co–Pd/Al_2O_3$	0.32	84.3

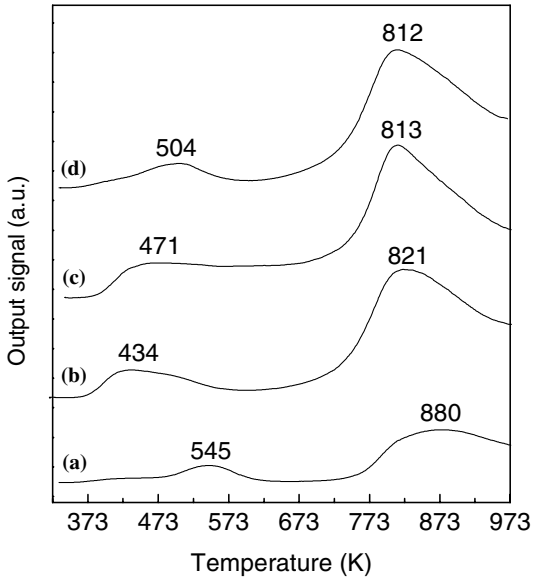

Figure 3. H_2-TPD patterns of the unpromoted and promoted catalysts. (a) Co/Al_2O_3; (b) $Co–Pt/Al_2O_3$; (c) $Co–Pd/Al_2O_3$; (d) $Co–Ru/Al_2O_3$.

It is obvious that the addition of noble metals to Co/Al_2O_3 led to some significant changes in H_2-TPD pattern. First, the addition of noble metals caused the peaks to shift markedly to lower temperatures. For low temperature peaks, the sequence of temperature decrease is $Co–Pt/Al_2O_3 > Co–Pd/Al_2O_3 > Co–Ru/Al_2O_3$, and more than 110 K decrease was observed for Pt-promoted catalyst. For high temperature peaks, the temperature decreases, however, are nearly the same. The marked temperature decrease of the low temperature peak indicates that the bond strength of Co–H on these promoted catalysts was significantly weakened. The relatively weaker Co–H bonding can facilitate the transfer of the adsorbed hydrogen species to the CO molecules adsorbed on the neighboring Co active sites, thereby enhancing the hydrogenation reactions. Second, the promoted catalysts exhibited rather higher amount of desorbed hydrogen than the unpromoted Co/Al_2O_3. There is no doubt that the increase of chemisorbed hydrogen on these promoted catalysts is mainly due to the improved reducibility. It is widely accepted that the rate determining step in CO-hydrogenation over Co catalyst is the hydrogenation of an activated carbon species [25,26]. Therefore, the enhancement in the amount of chemisorbed hydrogen is beneficial to improving the catalytic activity. In addition, the evident increase in the amount of high temperature desorption hydrogen provides the convincing evidence that hydrogen spillover from noble metals to the support, and subsequently to the remote cobalt oxide species during catalyst reduction, likely occurs. Because the FTS reaction with cobalt-based catalyst is usually conducted in the low temperature (473–513 K) range, it seems that the high temperature desorption hydrogen (spillover hydrogen) has little impact on the reaction. However, some authors [24] suggested that the spillover hydrogen can create active site on the silica where olefins can be hydrogenated to the corresponding paraffins. Whether the spillover hydrogen of the promoted Co/Al_2O_3

catalysts participates in the FTS reaction is not clear and further studies are necessary.

3.2.5. Temperature-programmed surface reaction

It is known that the chemisorption of CO on the catalyst under reaction conditions is strong and the coverage ratio is close to unity, whereas the chemisorption of H_2 is weak and the coverage is very low [27,28]. Therefore, the hydrogenation of chemisorbed CO is expected to be close to the catalytic hydrogenation of CO. Temperature-programmed surface reaction (TPSR) experiment was conducted in order to get a better insight into the nature of the active sites involved in the hydrogenation of chemisorbed CO.

The CH_4 TPSR profiles for the unpromoted and promoted Co/Al_2O_3 catalysts are shown in figure 4. For the unpromoted Co/Al_2O_3 catalyst, one single CH_4 peak at about 478 K was observed. The temperature at which methane started to be formed and the corresponding maximum shifted to lower temperatures when the noble metals were added to Co/Al_2O_3. It is suggested that the temperature of methane formation represents the reactivity of adsorbed CO [27]. Thus, the decrease in the CH_4 peak temperatures indicates that CO was adsorbed in a more reactive state on the promoted catalysts. In other words, the activity for hydrogenation of adsorbed CO is enhanced by noble metal promoters. It was also found that the Pt and Ru-promoted catalysts exhibit two resolved CH_4 peaks. For the promoted catalysts, the first peak temperatures follow the order: $Co–Ru/Al_2O_3 < Co–Pd/Al_2O_3 < Co–Pt/Al_2O_3$. This is very consistent with that reported for hydrogenation of adsorbed CO on alumina supported platinum group metals [27], indicating that the reactivity of adsorbed CO is greatly influenced by the noble metals even though the amount of promoter is small.

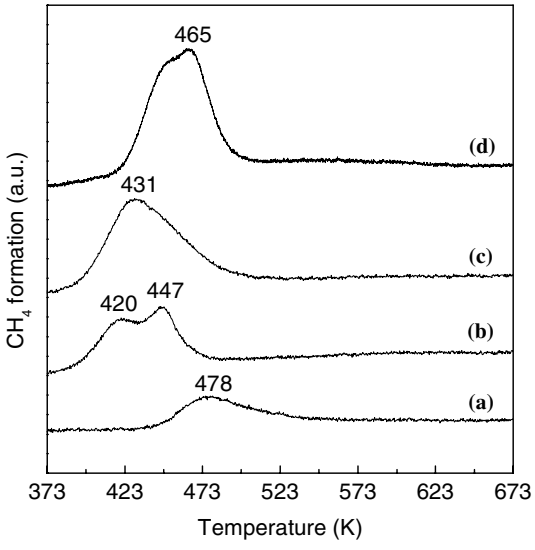

Figure 4. TPSR of adsorbed CO on the unpromoted and promoted Co/Al_2O_3 catalysts. (a) Co/Al_2O_3; (b)$Co–Ru/Al_2O_3$; (c) $Co–Pd/Al_2O_3$; (d) $Co-Pt/Al_2O_3$.

4. Conclusion

The addition of small amounts of noble metal (Pt, Pd or Ru) markedly decreased the reduction temperatures of both Co_3O_4 and cobalt surface species interacting with the support due to the hydrogen spillover effect evidenced by the TPR measurements. As a result, the reducibilities of these promoted catalysts increased remarkably. H_2-TPD results indicate that the amount of chemisorbed hydrogen was enhanced and the bond strength of Co–H was weakened after the addition of noble metals. TPSR results provide evidence that the reactivity of adsorbed CO can be increased by addition of noble metals. For these reasons, the overall catalytic activity of Co/Al_2O_3 catalyst in Fischer–Tropsch synthesis was significantly improved by noble metal addition.

References

[1] E. Iglesia, Appl. Catal. A 161 (1997) 59.
[2] S.A. Hosseini, A. Taeb, F. Feyzi and F. Yaripour, Catal. Comm. 5 (2004) 137.
[3] D.G. Wei, J.G. Goodwin Jr., R. Oukaci and A.H. Singleton, Appl. Catal. A 210 (2001) 137.
[4] A. Kogelbauer, J.G. Goodwin Jr. and R.J. Oukaci, J. Catal. 160 (1996) 125.
[5] A.M. Hilmen, D. Schanke and A. Holmen, Catal. Lett. 38 (1996) 143.
[6] L. Guczi, D. Bazin, I. Kovacs, L. Borko, Z. Schay, J. Lynch, P. Parent, C. Lafon, G. Stefler, Z. Koppany and I. Sajo, Top. Catal. 20 (2002) 129.
[7] T.K. Das, G. Jacobs, P.M. Patterson, W.A. Conner, J.L. Li and B.H. Davis, Fuel 82 (2003) 805.
[8] S. Vada, A. Hoff, E. Adnanes, D. Schanke and A. Holmen, Top. Catal. 2 (1995) 155.
[9] C.L. Bianchi, Catal. Lett. 76 (2001) 155.
[10] G. Jacobs, T.K. Das, Y.Q. Zhang, J.L. Li, G. Racoillet and B.H. Davis, Appl. Catal. A 233 (2002) 263.
[11] M.L. Jia, W.Z. Li, H.Y. Xu, S.F. Hou and Q.J. Ge, Appl. Catal. A 233 (2002) 7.
[12] S.L. Sun, N. Tsubaki and K. Fujimoto, Appl. Catal. A 202 (2000) 121.
[13] R.D. Jones and C.H. Barthoholomew, Appl. Catal. A 39 (1988) 77.
[14] D. Schanke, S. Vada, E.A. Blekkan, A.M. Hilmen, A. Hoff and A. Hollmen, J. Catal. 156 (1995) 85.
[15] B. Jongsomjit, J. Panpranot and J.G. Goodwin Jr., J. Catal. 204 (2001) 98.
[16] G. Jacobs, T.K. Das, P.M. Patterson, J.L. Li, L. Sanchez and B.H. Davis, Appl. Catal. A 247 (2003) 335.
[17] W.J. Wang and Y.W. Chen, Appl. Catal. A 77 (1991) 223.
[18] R.L. Chin and D.M. Hercules, J. Phys. Chem. 86 (1982) 360.
[19] E. Iglesia, S.L. Soled, R.A. Fiato and G.H. Via, J. Catal. 143 (1993) 345.
[20] A.M. Hilmen, D. Schanke, K.F. Hanssen and A. Holmen, Appl. Catal. A 186 (1999) 169.
[21] M. Reinikainen, M.K. Niemelä, N. Kakuta and S. Suhonen, Appl. Catal. A 174 (1998) 61.

[22] J.T. Miller, B.L. Meyers, M.K. Barr, F.S. Modica and D.C. Koningsberger, J. Catal. 159 (1996) 41.
[23] A. Bernas, N. Kumar, Mäki-Arvela Päivi, N.V. Kul'kova, B. Holmbom, T. Salmi and D.Y. Murzin, Appl. Catal. A 245 (2003) 257.
[24] M. Ojeda, M. López Granados, S. Rojas, P. Terreros and J.L.G. Fierro, J. Mol. Catal. A 202 (2003) 179.
[25] B.W. Wojciechowski, Catal. Rev. Sci. Eng. 30 (1988) 629.
[26] M.E. Dry, Catal. Today 6 (1990) 183.
[27] K. Fujimoto, M. Kameyama and T. Kunugi, J. Catal. 61 (1980) 7.
[28] G.P. Van der Laan and A.A.C.M. Beenackers, Catal. Rev.-Sci. Eng. 41 (1999) 255.